

A&A manuscript no.
(will be inserted by hand later)

Your thesaurus codes are:

1 (13.07.2; 02.14.1; 08.09.2 γ^2 Vel; 08.23.2; 09.09.1 IRAS Vela shell)

ASTRONOMY
AND
ASTROPHYSICS

COMPTEL limits on ^{26}Al 1.809 MeV line emission from γ^2 Velorum

U. Oberlack^{1,6}, U. Wessolowski¹, R. Diehl¹, K. Bennett⁴, H. Bloemen², W. Hermsen², J. Knödlseider⁵, D. Morris³, V. Schönfelder¹, and P. von Ballmoos⁵

¹ Max-Planck-Institut für extraterrestrische Physik, D-85740 Garching, Germany

² SRON Utrecht, NL-3584 CA Utrecht, The Netherlands

³ Space Science Center, University of New Hampshire, Durham NH 03824, USA

⁴ Astrophysics Division, ESTEC, NL-2200 AG Noordwijk, The Netherlands

⁵ Centre d'Etude Spatiale des Rayonnements (CNRS/UPS), F-31028 Toulouse, France

⁶ Columbia Astrophysics Laboratory, Columbia University, New York NY 10027, USA

Received ...; accepted October 28, 1999

Abstract. The Wolf-Rayet binary system γ^2 Vel (WR 11) is the closest known Wolf-Rayet (WR) star. Recently, its distance has been redetermined by parallax measurements with the HIPPARCOS astrometric satellite yielding 258_{-31}^{+41} pc, significantly lower than previous estimates (300 – 450 pc). Wolf-Rayet stars have been proposed as a major source of the Galactic ^{26}Al observed at 1.809 MeV. The gamma-ray telescope COMPTEL has previously reported 1.8 MeV emission from the Vela region, yet located closer to the Galactic plane than the position of γ^2 Vel. We derive an upper 1.8 MeV flux limit of $1.1 \cdot 10^{-5} \gamma \text{ cm}^{-2} \text{ s}^{-1}$ (2σ) for the WR star. With the new distance estimate, COMPTEL measurements place a limit of $(6.3_{-1.4}^{+2.1}) \cdot 10^{-5} M_{\odot}$ on the ^{26}Al yield of γ^2 Vel, thus constrains theories of nucleosynthesis in Wolf-Rayet stars. We discuss the implications in the context of the binary nature of γ^2 Vel and present a new interpretation of the IRAS Vela shell.

Key words: Gamma rays: observations – Nucleosynthesis – Stars: Wolf-Rayet – Stars: individual: γ^2 Vel – ISM: individual objects: IRAS Vela shell

1. Introduction

The 1.809 MeV gamma-ray line from radioactive decay of ^{26}Al [mean lifetime $(1.07 \pm 0.04) \cdot 10^6$ yr (Endt 1990)] traces recent nucleosynthesis in the Galaxy. This was the first gamma-ray line detected from the interstellar medium (Mahoney et al. 1984), and had been predicted from nucleosynthesis calculations of explosive carbon burning in core-collapse supernovae (Ramaty & Lingenfelter 1977; Arnett 1977). Other ^{26}Al production sites have been proposed as well, covering a wide range of densities ($0.5 - 3 \cdot 10^5 \text{ g cm}^{-3}$), temperatures ($3 \cdot 10^7 - 3 \cdot 10^9$ K), and time scales ($1 - 10^{14}$ s) at which proton capture on ^{25}Mg (within the Mg-Al chain) would create ^{26}Al : explosive hydrogen burning in novae and supernovae (Arnould et al.

1980), neon burning in the presupernova and supernova stage (e.g. Woosley & Weaver 1995), neutrino-induced nucleosynthesis in supernovae (Woosley et al. 1990), convective core hydrogen burning in very massive stars (Dearborn & Blake 1985), and hydrogen shell burning or “hot bottom burning” at the base of the convective stellar envelope in asymptotic giant branch (AGB) stars (Nørgaard 1980; Forestini et al. 1991). ^{26}Al nucleosynthesis and observations have been reviewed by Clayton & Leising (1987); MacPherson et al. (1995); Prantzos & Diehl (1996); Diehl & Timmes (1998).

Current theories still predict significant amounts of ^{26}Al from core-collapse supernovae (Woosley & Weaver 1995; Thielemann et al. 1996; Timmes et al. 1995), the wind phases of very massive stars where ^{26}Al is produced on the main sequence and ejected mainly in the Wolf-Rayet stage (Langer et al. 1995; Meynet et al. 1997) or possibly (in case of fast rotating stars) in a red supergiant stage as well (Langer et al. 1997), and from the most massive AGB stars (Bazán et al. 1993). The expected ^{26}Al contribution of chemically enriched novae lowered after major revisions of key reaction rates (José et al. 1997; Starrfield et al. 1998). All models suffer from large uncertainties in ^{26}Al yields, ranging from factors of three to orders of magnitude for the various proposed astrophysical sites.

Recent results from the COMPTEL telescope aboard the Compton Gamma-Ray Observatory showed growing evidence for a young (massive) population dominating the galaxy-wide ^{26}Al production (Diehl et al. 1995b; Knödlseider et al. 1996b; Oberlack et al. 1996; Oberlack 1997; Knödlseider 1997). While low-mass AGB stars and novae can be ruled out as the main ^{26}Al source, a distinction between supernovae and hydrostatic production in very massive stars appears difficult due to the similar evolutionary time scales involved.¹ Therefore, detection of individual objects would be essential as calibrator, but the sensitivity of current instruments restricts this approach to very few objects. Upper limits for five individual supernova remnants have been derived by Knödlseider et al. (1996a) and

Send offprint requests to: Uwe Oberlack

Correspondence to: oberlack@astro.columbia.edu

¹ See Knödlseider (1999) for arguments favouring WR stars as the dominant source of Galactic ^{26}Al .

the possibility of interpreting 1.8 MeV emission from the Vela region with individual objects has been discussed by Oberlack et al. (1994) and Diehl et al. (1999).

γ^2 Vel (WR 11, van der Hucht et al. 1981) is a WC8+O8–8.5III binary system at $(l, b) = (262.8^\circ, -7.7^\circ)$, containing the nearest Wolf-Rayet star to the Sun at a distance of 258^{+41}_{-31} pc, as determined by parallax measurements with the HIPPARCOS satellite (van der Hucht et al. 1997; Schaerer et al. 1997). [Another recent investigation determines a spectral type of O7.5 for the O star (De Marco & Schmutz 1999).] A previous 1.8 MeV flux limit (2σ) for γ^2 Vel of $1.9 \cdot 10^{-5} \gamma \text{ cm}^{-2} \text{ s}^{-1}$ had been determined by Diehl et al. (1995a), based on observations of the first 2 1/2 CGRO mission years.

In Sect. 2, we describe our search for 1.8 MeV emission from γ^2 Vel and the derivation of upper flux limits for several emission models. Sect. 3 discusses the initial mass range of the WR star, implications of our flux limit for stellar models, and proposes an alternative interpretation of the “IRAS Vela shell”. We summarize in Sect. 4.

2. Data analysis and source models

The COMPTEL telescope spans an energy range from 0.75 to 30 MeV with spectral resolution of 8% (FWHM) at 1.8 MeV, and performs imaging with an angular resolution of 3.8° FWHM at 1.8 MeV within a ~ 1 sr field of view. It features the Compton scattering detection principle through a coincidence measurement in two detector planes (see Schönfelder et al. (1993) for details). Imaging analysis and model fitting occurs in a three-dimensional dataspace consisting of angles $(\chi, \psi, \bar{\varphi})$ describing the scattered photon’s direction and the estimated Compton scatter angle, respectively (Diehl et al. 1992).

In this paper, we concentrate on fitting sky models, convolved with the instrumental response, in the imaging dataspace. The present analysis makes use of all data from observations 0.1 – 522.5 which have been combined in a full-sky dataset, comprising 5 years of observing time between May 1991 and June 1996. Events were collected within a 200 keV wide energy window from (1.7 – 1.9) MeV into the imaging dataspace with $1^\circ \times 1^\circ$ binning in (χ, ψ) (in galactic coordinates) and 2° binning in $\bar{\varphi}$. The dataspace has been restricted to $l \in [185^\circ, 320^\circ]$ and $|b| \leq 50^\circ$ to concentrate on emission from the Vela region, but not to loose information from the up to 100° wide response cone (at $\bar{\varphi} = 50^\circ$). The instrumental and celestial continuum background have been modelled by interpolation from adjacent energies, with enhancements from Monte Carlo modelling of identified activation background components. A previous version of the background handling and event selections have been described by Oberlack et al. (1996) and Knödlseider et al. (1996c), more details on the recently improved background handling and the complete dataset are reported in Oberlack (1997) [Oberlack et al., in prep.].

For the derivation of upper limits, the maximum likelihood ratio test has been applied (Cash 1979): A null hypothesis H_0 is compared with an extended alternative hypothesis H_1 , which includes q additional continuous model parameters, using the

likelihood function \mathcal{L} , which is the product of the Poisson probabilities p_k in N dataspace cells:

$$\mathcal{L} = \prod_{k=1}^N p_k \quad p_k = \begin{cases} \frac{\mu_k^{n_k}}{n_k!} e^{-\mu_k} & \text{for } \mu_k > 0 \\ 1 & \text{for } \mu_k = 0, n_k = 0 \\ 0 & \text{for } \mu_k = 0, n_k > 0 \end{cases} \quad (1)$$

where n_k is the number of counts in cell k and

$$\mu_k = \sum_{s=1}^{n_{\text{src}}} a^{(s)} \mu_k^{(s)} + b \mu_k^{\text{bgd}} \quad (2)$$

is the predicted number of counts due to sources and the background model, which includes the scaling parameters $a^{(s)}$, b varied in the fit. Each source model (s) can be described by a (normalized) flux map $\{f_j^{(s)}\}$ convolved with the response matrix R_{jk} :

$$\mu_k^{(s)} = \sum_j R_{jk} f_j^{(s)} \quad (3)$$

If the null hypothesis is true, the probability distribution of the ratio of the maximum likelihood $\hat{\mathcal{L}}_1$ achieved by fitting H_1 to the data over the maximum likelihood $\hat{\mathcal{L}}_0$ achieved by fitting H_0 to the data can be described analytically:

$$p \left(2 \ln \left(\frac{\hat{\mathcal{L}}_1}{\hat{\mathcal{L}}_0} \right) \right) = p(\chi_q^2) \quad (4)$$

where $p(\chi_q^2)$ is the tabulated χ^2 probability distribution with q degrees of freedom.

Fig. 1 shows a Maximum-Entropy deconvolved map of the 1.8 MeV emission from the Carina / Vela / Puppis regions. While no 1.8 MeV flux is detected from the position of γ^2 Vel, significant extended emission is observed in nearby regions, with an intensity peak around $(267^\circ.5, -0^\circ.5)$. Due to the broad COMPTEL response, such emission needs to be modelled. We test its impact on flux limits for γ^2 Vel with four different emission models (additional to the background model), guided by the deconvolved image, by candidate ^{26}Al sources in the region, and by results on the galaxy-wide ^{26}Al distribution. These are the tested source models in addition to the background model:

- A single point source at the position of γ^2 Vel.
- A detailed model describing the observed emission empirically and including 1.8 MeV candidate sources of the region (Fig. 1): an exponential disk with emissivity $\propto \exp\{-R/R_0\} \cdot \exp\{-|z|/z_0\}$, galactocentric scale length $R_0 = 4$ kpc, and scale height $z_0 = 180$ pc as an approximation to the large-scale ^{26}Al distribution, an additional homogenous stripe around $l = 310^\circ$ for simplified modelling of excess emission in this region and 8 point sources including γ^2 Vel. Details are listed in Table 1.
- An intermediate model: 2 point sources at the positions of maximum intensity in Fig. 1 at (l, b) : $(286^\circ.0, 0^\circ.0)$, $(267^\circ.5, -0^\circ.5)$ plus a point source for γ^2 Vel.

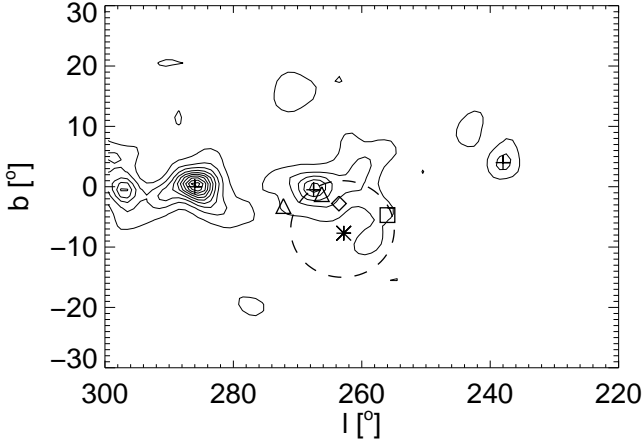


Fig. 1. COMPTEL 1.8 MeV map of the Carina / Vela / Puppis regions based on a deconvolution using the Maximum Entropy Method (Oberlack 1997). Contour lines are equally spaced with steps of $2.9 \cdot 10^{-4} \gamma \text{ cm}^{-2} \text{ s}^{-1} \text{ sr}^{-1}$. The dashed line indicates the IRAS Vela shell, the marked point source models are listed in Table 1.

Exponential disk:	$R_0 = 4 \text{ kpc}, z_0 = 180$	
Homogenous stripe:	$300^\circ \leq l \leq 320^\circ \quad b \leq 3^\circ$	
Point sources (l, b)		
* ($262^\circ.8, -7^\circ.7$) γ^2 Vel	+	($238^\circ.0, 4^\circ.0$) Puppis feature
□ ($256^\circ.0, -4^\circ.7$) ζ Pup	◇	($263^\circ.6, -2^\circ.8$) Vela pulsar
△ ($266^\circ.2, -1^\circ.2$) SNR “Vela Junior” [§]	+	($267^\circ.5, -0^\circ.5$) Vela feature
△ ($272^\circ.2, -3^\circ.2$) SNR G272.2 – 3.3	+	($286^\circ.0, 0^\circ.0$) Carina feature

Table 1. Source components of the detailed model (b). For the exponential disk, scale length and scale height are given as well as the range of the homogenous stripe. Point sources reflect candidate ^{26}Al sources in the region and additional emission features appearing in the map. [§]Aschenbach (1998); Iyudin et al. (1998)

- d. Like model (c) but replacing the point source for γ^2 Vel by a model for the IRAS Vela Shell: a spherical shell with a thickness of 10% of the 8° radius around $(l, b) = (263^\circ, -7^\circ)$ (Sahu & Blaauw 1993).

The first three models assume that all ^{26}Al from γ^2 Vel is kept within an observed ‘ejecta-type’ wind shell around the binary system with a diameter of $57'$ (Marston et al. 1994). Given COMPTEL’s angular resolution, this can be modelled by a point source. For completeness, we consider a fourth model, which places ^{26}Al into the so-called IRAS Vela shell, an extended ($\sim 8^\circ$ radius) structure almost centered on γ^2 Vel, which has been identified by Sahu (1992) from IRAS $25\mu\text{m}$ – $100\mu\text{m}$ maps and investigations of cometary globules. This is a region of relatively bright $\text{H}\alpha$ emission within the Gum nebula (Chanot & Sivan 1983), where young stellar objects are forming (Prusti et al. 1992). Sahu found the Vela shell to be a structure distinct from the Gum nebula and presented an interpretation as supershell from the aged Vela OB2 association of which γ^2 Vel may be a member (de Zeeuw et al. 1997). (As a consequence of HIPPARCOS parallaxes, γ^2 Vel would be located on the very near side of the association.) In this case, part

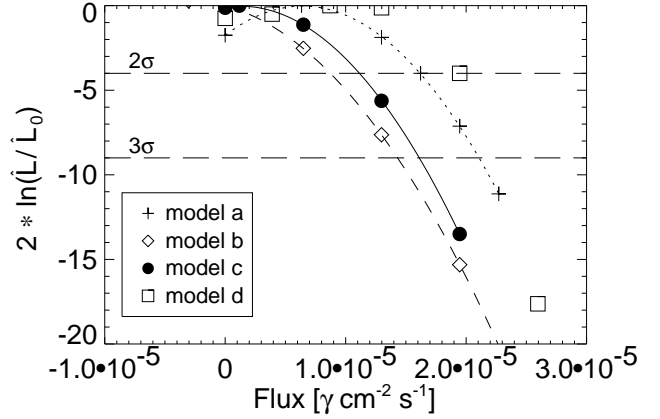


Fig. 2. Determination of upper flux limits with the maximum likelihood ratio test using 4 different emission models (see text).

of the ejected ^{26}Al may have traversed the gas bubble and be accumulated in the dense outer shell. We discuss a different interpretation, however, in Section 3.1.

Fig. 2 shows the logarithmic maximum likelihood ratio $2 \ln(\hat{L}/\hat{L}_0)$ as a function of model flux. No significant flux from γ^2 Vel is found for any of the tested models. The following 2σ upper limits are derived:

- Model a: $f < 1.6 \cdot 10^{-5} \gamma \text{ cm}^{-2} \text{ s}^{-1}$
 Model b: $f < 0.9 \cdot 10^{-5} \gamma \text{ cm}^{-2} \text{ s}^{-1}$
 Model c: $f < 1.1 \cdot 10^{-5} \gamma \text{ cm}^{-2} \text{ s}^{-1}$
 Model d: $f < 1.9 \cdot 10^{-5} \gamma \text{ cm}^{-2} \text{ s}^{-1}$

Given our 1.8 MeV map of the region, model (a) seems overly simplistic. Lacking alternative source models, part of the observed Vela emission is attributed to γ^2 Vel and yields the most conservative upper limit for a point source model. Model (b) contains many free parameters and may approach an over-fit of the data, where statistical fluctuations of the background are fitted. Although the fitted background scaling factor is lowest for this model, the lowest (even slightly negative) flux is attributed to γ^2 Vel. Consistent with the map in Fig. 1, the flux from Vela-Puppis is better described by sources within the galactic plane than by γ^2 Vel. Model (c) is “intermediate” in that it accounts for the strongest features in the map with a minimum of free model parameters. We adopt its result for the γ^2 Vel flux limit and consider models (a) and (b) as the extreme values for the systematic uncertainty due to the choice in modelling of other emission close ($\sim 5^\circ - 10^\circ$) to γ^2 Vel. The limit from model (d) is highest due to the large extent of this source model. Yet, we do not consider this model a likely representation of ^{26}Al from γ^2 Vel, even if the structure itself may well be related to the binary system, as discussed in the next section.

The 1.8 MeV flux directly translates into the “alive” ^{26}Al mass in the circumstellar medium, for a point source via:

$$f_{1.8 \text{ MeV}} = 1.8 \cdot 10^{-5} \gamma \text{ cm}^{-2} \text{ s}^{-1} \cdot \left(\frac{258}{d [\text{pc}]} \right)^2 \cdot \frac{M_{26} [M_\odot]}{1.0 \cdot 10^{-4}}$$

Therefore, our 2σ upper flux limit corresponds to a maximum ^{26}Al mass from γ^2 Vel of

$$M_{26}^{\text{WR11}} < (6.3_{-1.4}^{+2.1}) \cdot 10^{-5} M_{\odot} \quad (5)$$

where the 1σ distance uncertainties from the HIPPARCOS measurement have been taken into account.

3. Discussion

3.1. Interpretation of the IRAS Vela shell

Is our upper limit for the ^{26}Al yield from γ^2 Vel realistic, being derived for a point source model, or should we rather consider the higher value implied by potential ^{26}Al accumulation in the IRAS Vela shell?

The refined distance of γ^2 Vel suggests a new interpretation of the IRAS Vela shell as the *main sequence bubble* of the WR progenitor star in the γ^2 Vel system. This would make a significant ^{26}Al contamination of the shell unlikely since this isotope is expected to appear at the stellar surface only in later stages of stellar evolution, together with the products of core hydrogen burning, after the hydrogen shell has been expelled. Evidence for our interpretation stems from observations of interstellar reddening by Franco (1990), who studied two regions within the Gum nebula, one of which in projection to the IRAS shell. Only this field showed clear evidence for a dust wall at a distance of 200 ± 20 pc, interpreted by the authors as the near edge of the Gum nebula. If this is now interpreted as the near edge of the IRAS shell, its angular extent would correspond to a radius of 32 pc and the centre would be placed at a distance of 230 ± 20 pc, well within the 1σ uncertainty of the γ^2 Vel distance. This would argue against a supershell interpretation since the distance to the centre of Vela OB2, the assumed origin of the supershell, has been precisely measured by HIPPARCOS to 415 ± 10 pc (de Zeeuw et al. 1997). Scaling down the (uncertain) mass estimate for the shell by Sahu from the distance of 450 pc she assumed to the reduced distance of γ^2 Vel, yields a mass of $\sim 2 \times 10^5 M_{\odot}$. Combined with the observed expansion velocity of $\sim 10 \text{ km s}^{-1}$ (Sahu & Sahu 1993) this corresponds to a kinetic energy of $\sim 2 \times 10^{43} \text{ J}$ ($2 \times 10^{50} \text{ erg}$), within the range of stellar wind energy release by a massive star. In a hydrodynamic model coupled with a stellar evolution code for a $60 M_{\odot}$ star, Garcia-Segura et al. (1996) even find a total energy release of $3.3 \times 10^{44} \text{ J}$ (70% - 80% thereof ejected before a “luminous blue variable” [LBV] phase) with a 45 pc radius O-star bubble. This number only scales weakly with ambient density ($\propto n^{-1/5}$, $n = 20 \text{ cm}^{-3}$ assumed in the model), but is considered an upper limit by the authors because effects like heat conduction or cloud evaporation are ignored here. Within the uncertainties of the model, our interpretation of the IRAS Vela shell seems therefore plausible. For the further discussion we will hence adopt our 1.8 MeV mass limit which was derived from the assumption that all ^{26}Al from γ^2 Vel is contained within a region of $\sim 1^\circ$ in diameter around γ^2 Vel.

3.2. Current mass estimate for γ^2 Vel

Model predictions of ^{26}Al yields for massive stars are a strong function of initial stellar mass, e.g., $M_{26} \propto M_1^{2.8}$ (Meynet et al. 1997). A direct determination of the WR star initial mass (and thus its predicted ^{26}Al yield) from comparison of luminosity and effective temperature with stellar evolution tracks, as is typically done for other types of stars, is not feasible due to the lack of sufficiently accurate models of WR wind atmospheres (and the additional complications from the binary nature of this stellar system). While binarity makes modeling more complicated due to additional degrees of freedom in parameter space it allows measurement of current masses, which can be matched with theoretical predictions together with the generic spectral type of the WR star. Spectroscopic determination of $M_{1,2} \sin^3 i$ (where i is the inclination) based on Doppler-shifted absorption (O star) and emission lines (WR star) led to contradictory results (Pike et al. 1983; Moffat et al. 1986). A recent redetermination of orbital parameters by Schmutz et al. (1997) yields spectroscopic masses of:

$$M_{\text{WR}} \sin^3 i = 6.8 \pm 0.6 M_{\odot} \quad M_{\text{O}} \sin^3 i = 21.6 \pm 1.1 M_{\odot}$$

They reject an earlier inclination measurement from polarisation data of $i = 70^\circ \pm 10^\circ$ by St.-Louis et al. (1988) and rather state wider inclination limits of $57^\circ < i < 86.3^\circ$ from other evidence, corresponding to a factor $1/\sin^3 i = 1.0 - 1.7$ or a range from 6 to $12 M_{\odot}$ for the current mass of the WR star. Relying on a mass-luminosity relation for the O star from *single* star evolution models, Schaerer et al. (1997) derive $M_{\text{O}} = 29 \pm 4 M_{\odot}$, which, in turn, yields a consistent, but model-dependent, inclination estimate of $i = 65^\circ \pm 8^\circ$ or a mass estimate for the WR star of $M_{\text{WR}} = 9_{-1.2}^{+2.5} M_{\odot}$ (Schmutz et al. 1997). A different analysis of the same spectral data yields a slightly higher luminosity for the O star, leading to a slightly higher O star mass estimate of $30 \pm 2 M_{\odot}$ (De Marco & Schmutz 1999), yet, with the same mass-luminosity relation from single-star models.

Another observational hint on the total mass of the binary system has been derived from interferometric measurements of the major half-axis of the binary system $a'' = (4.3 \pm 0.5) \text{ mas}$ by Hanbury Brown et al. (1970). Kepler’s law leads to a consistent, but barely constraining, mass estimate:

$$M_{\text{WR}} + M_{\text{O}} = \frac{(2\pi)^2 (a'' \cdot d)^3}{G T^2} = (30 \pm 16) M_{\odot} \quad (6)$$

The large relative uncertainty in total mass of $\sim 54\%$ is due to the uncertainties in a'' and d to about equal amounts. Additional systematic errors, however, may affect the determination of a'' by a fit in which other quantities like orbital parameters, inclination, and brightness ratio of the two stars had to be taken as fixed parameters due to limited data quality. Those values were taken from other measurements available at the time. Most notably, an eccentricity of 0.17 had been assumed which is distinctly lower than a recent value of 0.326 ± 0.01 (Schmutz et al. 1997). Future interferometric measurements could improve this situation significantly.

3.3. Single star models

Given the remaining uncertainties in current mass determinations, not surprisingly *initial* mass estimates and predicted ^{26}Al yields vary significantly. To start with the simpler case, we first discuss our results in the context of single star models, assuming that the stellar structure of the primary (defined in terms of which star evolved first, i.e. now the WR star) has not been significantly altered due to the presence of its binary companion and that all of the mass expelled from the primary has reached the ISM without being captured by the secondary. This corresponds to fully non-conservative mass transfer, which is usually parametrized by the fraction β of mass that is accreted by the secondary out of the mass lost by the primary (i.e. fully non-conservative mass transfer means $\beta = 0$). For the Geneva single star models, a minimum initial mass of about $40 M_\odot$ is required at solar metallicities to yield a WC-type Wolf-Rayet star (Meynet et al. 1994) as observed in γ^2 Vel. Therefore, these models would predict a minimum ^{26}Al yield of $5.5 \times 10^{-5} M_\odot$ for γ^2 Vel with initial mass of the WR component $M_i = 40 M_\odot$ and even $1.2 \times 10^{-4} M_\odot$ for $M_i = 60 M_\odot$, the value used by Meynet et al. (1997) for the description of γ^2 Vel. These yields are consistent with the yields predicted by the single-star models of Langer et al. (1995). Schaerer et al. (1997) estimate an initial mass of $M_i = 57 \pm 15 M_\odot$ for the WR star, using the Geneva models.

Has all ^{26}Al been expelled yet or is some fraction still buried invisibly inside the star? The spectral type of the Wolf-Rayet star is WC, i.e. the stellar wind is carbon rich, which means that products of core helium burning have reached the stellar surface. Since remaining ^{26}Al in the stellar core is efficiently destroyed in helium burning due to neutron captures, standard stellar evolution models predict that the wind ejection phase of hydrostatically produced ^{26}Al has ended already.

How much ^{26}Al has already decayed? Typical WR lifetimes from observational constraints and theoretical models are on the order of $\lesssim 5 \times 10^5$ yr, which is shorter than the ^{26}Al lifetime by a factor of 2. This could account for a reduction of observable ^{26}Al in the ISM of at most 40% if the WR star were close to the end of its evolution. Some models predict WR lifetimes in excess of a million years for the most massive stars (Meynet et al. 1997) but these models also predict sufficiently large ^{26}Al yields such that the prolonged time available for decay would not reduce the observable amount below the measured limit. Also note that WR lifetimes strongly depend on the mass loss description applied in the model.

A straight-forward explanation for the missing 1.8 MeV flux would be sub-solar metallicity since the ^{26}Al yields scale approximately like Z^2 . Yet, sub-solar abundances in the ISM observed in the Vela direction can readily be understood by dust formation (and therefore depletion of the gaseous phase) rather than by intrinsic low metallicity (Fitzpatrick 1996). Analysis of spectroscopic data for the O star in the binary system is indeed consistent with solar metallicity (De Marco & Schmutz 1999).

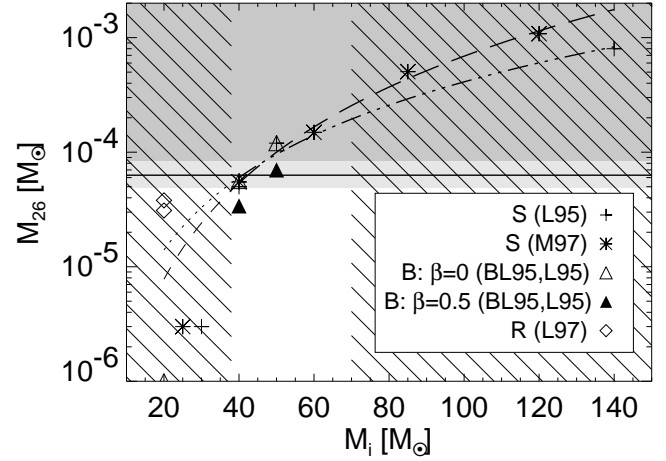


Fig. 3. ^{26}Al yields as a function of the initial mass of the WR component in the binary system. Plotted are single star (“S”) and binary (“B”) models as well as models of rotating (single) stars (“R”), all at solar metallicity. L95: Langer et al. (1995); M97: Meynet et al. (1997); BL95: Braun & Langer (1995); L97: Langer et al. (1997). For interpolation, the single star models were fitted with a power law (dashed and dash-dotted lines). The horizontal solid line marks our 2σ limit (using model c) for the ^{26}Al mass surrounding the WR star. The light-gray region corresponds to the 1σ distance uncertainty, the dark-gray region is excluded by the 1.8 MeV flux limit. The high-lighted area indicates the most probable initial mass range. Single star models are barely compatible with our measurement, and even binary models are consistent only at the lowest allowed initial mass range and would require significant mass transfer (β) from the primary to the secondary.

With these considerations, Fig. 3 shows that ^{26}Al yields predicted from single star models are barely compatible with the COMPTEL flux limit. This would suggest that model parameters such as the mass loss description, which has greatest impact on the stellar structure for initial masses $\gtrsim 40 M_\odot$, or internal mixing parameters like core overshooting or semi-convection may have to be modified.

3.4. Binary models

Differences in the stellar evolution of the primary star in a relatively wide binary system such as γ^2 Vel ($a \approx 1$ AU) stem from mass loss, while effects of tidal forces on the stellar structure are negligible during the main sequence phase when ^{26}Al is produced in the core. In addition to the mass loss mechanisms of single stars, Roche Lobe Overflow (RLOF) can change the stellar structure of both primary and secondary star. For the discussion of ^{26}Al yields, we can concentrate on the evolution of the primary since the secondary O star merely reveals unprocessed material from the stellar envelope at its surface, but might bury some of the processed material transferred from the primary. Langer (1995) proposes that binary stars with $M_i \gtrsim 40 M_\odot$ undergoing RLOF are essentially indistinguish-

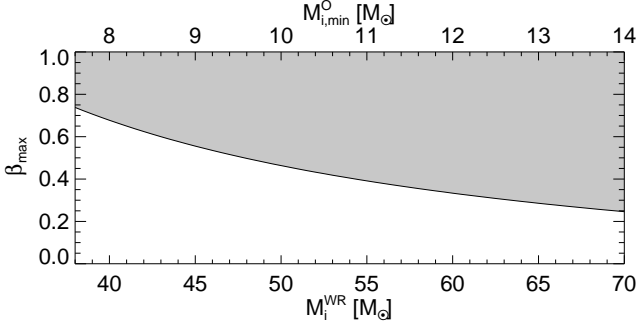


Fig. 4. Maximum value for the mass fraction β transferred to the secondary assuming current masses $M_{\text{WR}} = 9 M_{\odot}$, $M_{\text{O}} = 29 M_{\odot}$, and an initial mass ratio $q > 0.2$ to avoid merging (Vanbeveren et al. 1998).

able from single stars in the same mass range undergoing a phase of very intense mass loss as LBVs. Differences in the ^{26}Al yield in the circumstellar medium would merely result from the fraction of expelled mass captured by the secondary companion, i.e. some fraction $\lesssim \beta$ could be buried in the surface layers of the secondary. (Stellar winds from primary and secondary will always transport some fraction of ^{26}Al into the ISM.) Vanbeveren (1991) argues that this LBV mass loss may even prevent any occurrence of RLOF, which means that ^{26}Al yields should remain the same as for single stars.

For initial masses below $\sim 40 M_{\odot}$, RLOF can provide additional mass loss not attainable in the single star scenario, pushing down the lower initial mass limit for the formation of WR stars to about $20 M_{\odot}$ (Vanbeveren et al. 1998). Yet, adopting current masses of $9 M_{\odot}$ for the WR star and $29 M_{\odot}$ for the O star and assuming a fraction of mass transferred to the secondary as high as $\beta = 0.5$ would yield a minimum initial mass for the primary of $\sim 30 M_{\odot}$, given that the primary star must have been the more massive partner initially to evolve faster. The observed current mass loss rate of $(2.8^{+1.2}_{-0.9}) \times 10^{-5} M_{\odot}/\text{yr}$ (Schaerer et al. 1997), quite typical for this type of star, supports a minimum mass lost into the ISM of at least $10 M_{\odot}$ in the last few 100,000 years. Vanbeveren et al. (1998) quote a minimum initial mass of $38 M_{\odot}$ for the WC star in γ^2 Vel based on detailed models of binary evolution.

Overall, the minimum initial mass for the WR star in binary models is found close to the values obtained by single star models, namely around $40 M_{\odot}$. While the real initial mass may well have been larger, it is apparent from Fig. 3 that discrepancies between predicted ^{26}Al yields and the measured 1.8 MeV flux limit become quite severe for larger masses. Even for $M_i = 40 M_{\odot}$, models are in clearly better agreement with the flux limit if a significant fraction of the ejected mass of the primary accreted onto the secondary. The binary models of Braun & Langer (1995) lead to a typical reduction in ^{26}Al yield of about 40% for models with $\beta = 0.5$ as displayed in the figure.

Information regarding a quantitative estimate of β is still sparse, but some statements can be made. If we consider $M_i \approx$

$40 M_{\odot}$ the lowest possible initial mass for the WR star, the fact that binaries with initial mass ratios (secondary / primary) $q < 0.2$ are expected to merge (Vanbeveren et al. 1998) leads to a minimum initial mass for the O star of $\sim 8 M_{\odot}$, hence an initial total mass of the system of $\gtrsim 48 M_{\odot}$. Assuming a current mass of $(29 + 9 = 38) M_{\odot}$ as for the initial mass estimate, a minimum of $10 M_{\odot}$ must have been expelled to the ISM, while about $20 M_{\odot}$ would have been transferred to the secondary, corresponding to $\beta \approx 2/3$. Any larger value of q , i.e. larger initial mass of the O star, would yield lower β . For larger values of the initial mass of the WR star, the maximum allowed β for $q > 0.2$ rapidly decreases as illustrated in Fig. 4.

Observation of an “ejecta-type” ring nebula around γ^2 Vel with $57''$ angular diameter (Marston et al. 1994), corresponding to a radius of 2.1 pc, demonstrates that significant mass has been expelled from the system, probably during a preceding LBV / WN phase, even though the mass of the shell has not yet been determined. If indeed the IRAS Vela shell were the remnant of the main sequence bubble of the primary star, the mass transfer to the secondary would be negligible compared to the ejected mass and the WR star could be reasonably modeled by a $M_i \approx 60 M_{\odot}$ star (Garcia-Segura et al. 1996). This scenario is supported by the recent finding that the helium abundance in the companion O star is not enriched (De Marco & Schmutz 1999) as one might expect if significant amounts of processed material had been transferred to the secondary star. This, however, would imply a major conflict of the ^{26}Al yields predicted by corresponding stellar models with our measurement.

There are additional qualitative arguments for both *very little* mass transfer to the secondary but also *some* mass transfer: The relatively high excentricity of the orbit favours little mass transfer, which usually tends to reduce the excentricity. On the other hand, the high rotation velocity of the secondary of $v_{\text{rot}} \sin i = 220 \text{ km s}^{-1}$ (Baade et al. 1990) may be the result of spinning up by accretion. More detailed modeling is required to resolve these issues.

4. Conclusion

Given the small distance of γ^2 Vel from HIPPARCOS measurements and predicted ^{26}Al yields of current stellar models, the non-detection of 1.8 MeV emission by COMPTEL comes as a surprise. Combined with other observations regarding current masses, metallicity and mass transfer, only a very small volume of the model parameter space remains consistent with the COMPTEL 2σ upper limit of $M_{26}^{\text{WR11}} < (6.3^{+2.1}_{-1.4}) \cdot 10^{-5} M_{\odot}$. Single star models are in conflict with this value. Binary models alleviate the discrepancy if significant mass transfer to the secondary occurred, burying some fraction of ^{26}Al in the surface layers of the O star, and if the initial mass of the WR star was close to its minimum value of $\sim 40 M_{\odot}$. It may be more likely, however, that adjustment of some of the model parameters, e.g. the parametrization of mass loss, is required.

Unfortunately, γ^2 Vel is the only known WR star for which there was hope to obtain a positive detection with current instruments. The WR stars next closest to the Sun (WR142,

WR145, and WR147 in the Cygnus region) are at least a factor of two more distant, and therefore their expected fluxes are out of reach for COMPTEL. For the forthcoming INTEGRAL mission, these stars may just become detectable, and the 1.8 MeV flux from γ^2 Vel will be tested down to significantly lower values. Yet, to probe the 1.8 MeV flux from individual WR stars within the radius of completeness of the current WR catalogue ($\sim 2.5 - 3$ kpc), would require a next-generation instrument with a sensitivity of $10^{-7} \gamma \text{ cm}^{-2} \text{ s}^{-1}$ and an angular resolution $< 0.2^\circ$.

Acknowledgements. The COMPTEL project is supported by the German government through DARA grant 50 QV 90968, by NASA under contract NAS5-26645, and by the Netherlands Organization for Scientific Research NWO. The authors are grateful for discussions with Norbert Langer, Orsola De Marco, Georges Meynet, Tony Marston, Nikos Prantzos, Daniel Schaefer, and Werner Schmutz. We thank the referee Dieter Hartmann for helpful comments.

References

- Arnett W.D., 1977, in: Papagiannis D. (ed.), Eighth Texas Symposium on Relativistic Astrophysics, New York, vol. 302 of Ann. N.Y. Acad. Sci., p. 90
- Arnould M., Nørgaard H., Thielemann F.K., et al., 1980, ApJ 237, 931
- Aschenbach B., 1998, Nat 396, 141
- Baade D., Schmutz W., van Kerkwijk M., 1990, A&A 240, 105
- Bazán G., Brown L., Clayton D., et al., 1993, Rev. Mex. Astron. Astrofis. 27, 87
- Braun H., Langer N., 1995, in: van der Hucht K.A., Williams P.M. (eds.), Wolf-Rayet Stars: Binaries, Colliding winds, Evolution, Kluwer Academic Publishers, Dordrecht, IAU Symp. 163, pp. 305–308
- Cash W., 1979, ApJ 228, 939
- Chanot A., Sivan J.P., 1983, A&A 121, 19
- Clayton D.D., Leising M.D., 1987, Phys. Rep. 144, 1
- De Marco O., Schmutz W., 1999, A&A 345, 163
- de Zeeuw P.T., Brown A., de Bruijne J.H.J., et al., 1997, in: Perryman M.A.C., Bernacca P.L., Battrick B. (eds.), Proc. of the Hipparcos Venice 1997 Symp., SP-402, ESA
- Dearborn D.S.P., Blake J.B., 1985, ApJ 288, L21
- Diehl R., Timmes F.X., 1998, PASP 110, 637
- Diehl R., Aarts H., Bennett K., et al., 1992, in: Di Gesù V., Scarsi L., Buccheri R., et al. (eds.), Data Analysis in Astronomy IV, Plenum Press, New York, vol. 59 of Ettore Majorana Internat. Science Series
- Diehl R., Bennett K., Bloemen H., et al., 1995a, A&A 298, L25
- Diehl R., Dupraz C., Bennett K., et al., 1995b, A&A 298, 445
- Diehl R., Oberlack U., Plüschke S., et al., 1999, in: Palumbo G., Bazano A. (eds.), Third INTEGRAL Workshop, in press
- Endt P.M., 1990, Nucl. Phys. A 521, 1
- Fitzpatrick E.L., 1996, ApJ 473, L55
- Forestini M., Arnould M., Paulus G., 1991, A&A 252, 597
- Franco G.A.P., 1990, A&A 227, 499
- Garcia-Segura G., Mac Low M.M., Langer N., 1996, A&A 305, 229
- Hanbury Brown R., Davis J., Herbison-Evans D., et al., 1970, MNRAS 148, 103
- Iyudin A.F., Schonfelder V., Bennett K., et al., 1998, Nat 396, 142
- José J., Hernanz M., Coc A., 1997, ApJ 479, L55
- Knödlseeder J., 1997, Ph.D. thesis, Univ. Paul Sabatier, Toulouse, France
- Knödlseeder J., 1999, ApJ 510, 915
- Knödlseeder J., Oberlack U., Diehl R., et al., 1996a, A&AS 120, C339
- Knödlseeder J., Prantzos N., Bennett K., et al., 1996b, A&AS 120, C335
- Knödlseeder J., von Ballmoos P., Diehl R., et al., 1996c, in: Ramsey B.D., Parnell T.A. (eds.), Gamma-Ray and Cosmic-Ray Detectors, Techniques, and Missions, vol. 2806 of SPIE, p. 386
- Langer N., 1995, in: van der Hucht K.A., Williams P.M. (eds.), Wolf-Rayet Stars: Binaries, Colliding winds, Evolution, Kluwer Academic Publishers, Dordrecht, IAU Symp. 163, pp. 15–23
- Langer N., Braun H., Fliegner J., 1995, Ap&SS 224, 275
- Langer N., Fliegner J., Heger A., et al., 1997, Nucl. Phys. A 621, 457c
- MacPherson G.J., Davis A.M., Zinner E.K., 1995, Meteoritics 30, 365
- Mahoney W.A., Ling J.C., Wheaton W.A., et al., 1984, ApJ 286, 578
- Marston A.P., Yokum D.R., Garcia-Segura G., et al., 1994, ApJS 95, 151
- Meynet G., Maeder A., Schaller G., et al., 1994, A&AS 103, 97
- Meynet G., Arnould M., Prantzos N., et al., 1997, A&A 320, 460
- Moffat A.F.J., Paquin G., Lamontagne R., et al., 1986, AJ 91, 1386
- Nørgaard H., 1980, ApJ 236, 895
- Oberlack U., 1997, Ph.D. thesis, Technische Universität München, Germany
- Oberlack U., Diehl R., Montmerle T., et al., 1994, ApJS 92, 433
- Oberlack U., Bennett K., Bloemen H., et al., 1996, A&AS 120, C311
- Pike C.D., Stickland D.J., Willis A.J., 1983, Observatory 103, 154
- Prantzos N., Diehl R., 1996, Phys. Rep. 267, 1
- Prusti T., Adorf H.M., Meurs E.J.A., 1992, A&A 261, 685
- Ramaty R., Lingenfelter R.E., 1977, ApJ 213, L5
- Sahu M.S., 1992, Ph.D. thesis, Rijksuniversiteit Groningen, The Netherlands
- Sahu M.S., Blaauw A., 1993, in: Cassinelli J.P., Churchwell E.B. (eds.), Massive Stars: Their Lives in the Interstellar Medium, San Francisco, vol. 35 of ASP Conf. Ser., pp. 278–280
- Sahu M.S., Sahu K.C., 1993, A&A 280, 231
- Schaefer D., Schmutz W., Grenon M., 1997, ApJ 484, L153
- Schmutz W., Schweickhardt J., Stahl O., et al., 1997, A&A 328, 219
- Schönfelder V., Aarts H., Bennett K., et al., 1993, ApJS 86, 657
- St.-Louis N., Moffat A.F.J., Drissen L., et al., 1988, ApJ 330, 286
- Starrfield S., Truran J.W., Wiescher M.C., et al., 1998, MNRAS 296, 502
- Thielemann F.K., Nomoto K., Hashimoto M., 1996, ApJ 460, 408
- Timmes F.X., Woosley S.E., Hartmann D.H., et al., 1995, ApJ 449, 204
- van der Hucht K.A., Williams P.M. (eds.), 1995, Wolf-Rayet Stars: Binaries, Colliding winds, Evolution, IAU Symp. 163, Dordrecht, Kluwer Academic Publishers
- van der Hucht K.A., Conti P.S., Lundstrom I., et al., 1981, Space Science Reviews 28, 227
- van der Hucht K.A., Schrijver H., Stenholm B., et al., 1997, New Astron. 2, 245
- Vanbeveren D., 1991, A&A 252, 159
- Vanbeveren D., De Donder E., Van Bever J., et al., 1998, New Astron. 3, 443
- Woosley S.E., Weaver T.A., 1995, ApJS 101, 181
- Woosley S.E., Hartmann D.H., Hoffman R.D., et al., 1990, ApJ 356, 272